23rd International Conference
ENGINEERING MECHANICS 2017
Svratka, Czech Republic, 15 – 18 May 2017

MECHANICAL BEHAVIOR OF A TITANIUM ALLOY TRABECULAR STRUCTURE

L. Řehounek[*], A. Jíra[**], F. Denk[***]

Abstract: *The advancement of technology in the field of 3D printing of metal alloys allows for creating very complex structures. Newfound technologies of manufacturing, however, require testing of basic mechanical properties of the new structures. This paper is dedicated to the analysis of mechanical properties of a trabecular Ti-6Al-4V titanium alloy. Due to its complex morphology, the trabecular structure could not be created by traditional manufacturing process and was made by 3D printing. It was found that by creating this structure, the Young's modulus of the whole body of the specimen was significantly reduced. The methods used for the determination of the mechanical properties are nanoindentation, tensile and compression tests.*

Keywords: Trabecular, Nanoindentation, Modulus of elasticity, Titanium, 3D printing.

1. Introduction

A trustworthy representation of the behavior of the trabecular implant demands a detailed mathematical model representing the true stress-strain relation of the structure. Because of the nonlinear behavior and a yet unknown nature of deformation characteristics, it is imperative to provide a series of test data to serve as a guideline for the development of the model. The stress-strain relations have been provided by means of uniaxial tensile and compression tests. These tests have been carried out on specifically designed specimens shown in Fig. 1. The trabecular structure brings with itself many benefits, such as reduced risk of implant loosening (Dabrowski et al, 2010), osseointegration, complex implant integration and more acceptable (lower) values of Young's modulus, compared to other homogeneous implants (Niinomi, 1998 and Niinomi 1998). This reduction is a significant benefit because it provides a smoother transition region in between the faces of the dental materials. The trabecular structure also provides an environment into which bone cells are able to grow into, thus further improving the transition region and contact properties.The body of the implant has been 3D-printed using the M2 Cusing Concept Laser machine using a specialized Rematitan Cl metal powder in cooperation with ProSpon spol. s. r. o.

2. 3D printing technology

The first step in the process of creation of a 3D-printed product is creating a 3D-model. This part is usually done using a computer-aided design (CAD) environment. Upon its completion, an STL model file is divided into thin cross sections (Wiria et al., 2010 and Aouni et al., 2014) and sent to the 3D printer to be processed. Up to this point, the process is similar to the common layer-by-layer 3D-printing of plastic.

What differentiates the process of printing metals from the standard technology is using a laser beam to melt down a layer of metal powder, such as Rematitan Cl. During each cycle, the coater applies a thin layer of powder, which is processed by a laser at a pre-set melting point in a pre-determined order (Hartmann-H'Lawatscheck, 2015).

[*] Bc. Luboš Řehounek: Department of Mechanics, Czech Technical University in Prague, Thákurova 7; 166 29, Prague; CZ, lubos.rehounek@fsv.cvut.cz

[**] Ing. Aleš Jíra, PhD.: Department of Mechanics, Czech Technical University in Prague, Thákurova 7; 166 29, Prague; CZ, jira@fsv.cvut.cz

[***] Ing. arch. et Ing. František Denk, PhD.: Department of Mechanics, Czech Technical University in Prague, Thákurova 7; 166 29, Prague; CZ, frantisek.denk@fsv.cvut.cz

This process solidifies the loose powder into a 3D-layered object. 3D printing is a very modern and perspective method in manufacturing the bodies of the implants. It allows for very complex structures, which would not have been conceivable with traditional metalworking.

It also proves to be beneficial in terms of manufacturing speed and storage, because there is no need to produce large batches of specific implants at once due to the long process associated with the calibration of the assembly line.

a) compression test specimen b) tensile test specimen

Fig. 1: Trabecular structure specimens for global mechanical tests.

3. Methodology

3.1. Nanoindentation

To investigate the micromechanical properties of the alloy, nanoindentation tests were made considering reduced modulus of elasticity, hardness and contact depth. The micromechanical analysis was performed using the CSM Instruments nanoindenter in the mode of directed force and repeated loading. The load program was set with consideration of eliminating surface tension and shear stiffness in the atomic material structure. The values of reduced modulus E_r were in the range of 118 – 131 GPa. For further information about nanoindentation, please refer to the paper Řehounek et al. (2016).

3.2. Global mechanical tests

To investigate the global mechanical properties, we conducted compression and tensile tests. For this purpose, we used the 3D Dode-Thick [MSG] structures with dimensions of 14 × 14 × 14 mm (a cube for the compression test) and a 14 × 14 × 42 mm (a block for the tensile test). The tensile test specimen had a 14 mm trabecular middle section and end portions of homogeneous volume for ensuring a better anchor in the MTS Alliance RT-30 machine. The results show an ultimate compressive strength of 31.30 MPa and an ultimate tensile strength of 32.80 MPa. Diagram showing the stress-strain relations of the specimens obtained by tensile tests is shown in Fig. 2.

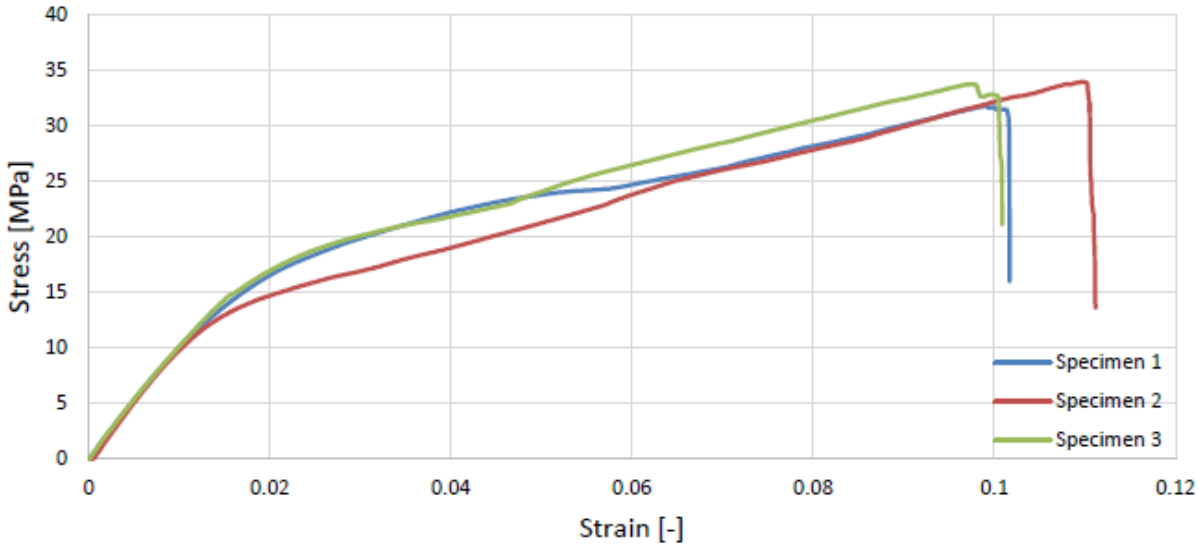

Fig. 2: Stress-strain relation diagram of the tensile test specimens.

From the linear part of the load curves of the tensile test diagram (as well as compression diagram, which was omitted for sake of brevity), we were able to calculate Young's modulus of the whole trabecular specimen (Tab. 1). These values represent properties of the whole specimen, contrary to the nanoindentation experiment, where obtained values represent only the material characteristics at the micro level.

Tab. 1: Values of Young's modulus obtained by global mechanical analysis.

	Young's modulus E [MPa]									
Specimen	1	2	3	4	5	6	7	8	9	Mean
Tens. test	964.7	975.9	982.2	-	-	-	-	-	-	**974.3**
Comp. test	-	-	-	1114.2	1080.6	947.2	818.8	999.6	803.8	**960.7**

4. FEM model

With the experimental data obtained, the next task was to develop a corresponding FEM model. Our first step in approaching the problem was to create a 3D geometry that represents the specimen.

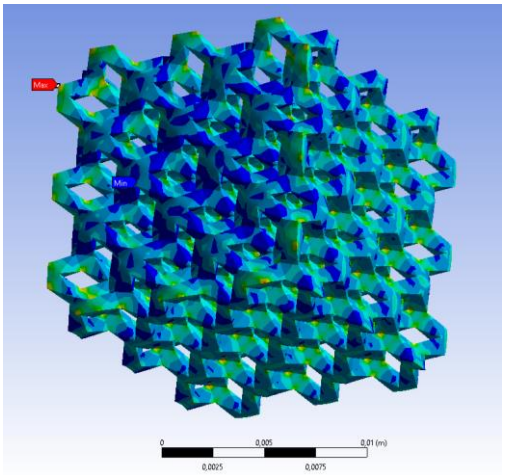

Fig. 3: Geometry of the FEM model under displacement load, isolines show strain distribution.

The software used for the purpose of computation is Workbench 16.2. of the ANSYS company. A custom material with nonlinear behavior was introduced and its parameters experimentally manipulated in order to ensure a real representation of the trabecular structure. Due to a rather chaotic nature of compressive deformation, the tensile test results have been chosen as a baseline for the curve fitting process.

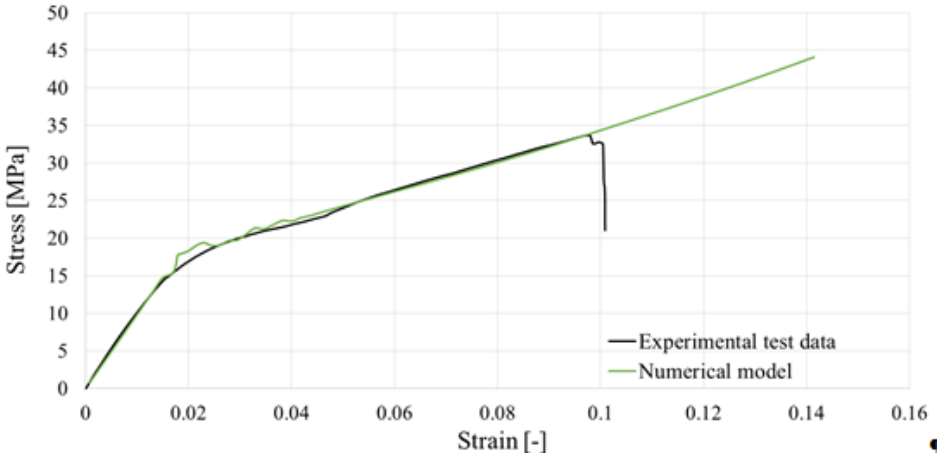

Fig. 4: Stress-strain relation diagram of the curve-fitted FEM model. Parameters successfully curve-fitted up until the area of structure failure.

The diagram shown in Fig. 4 represents the stress-strain relation of the curve-fitted FEM model. The main task was to manipulate its mechanical properties in order to curve-fit the tensile test experiment data of specimen n.3. This has been done by importing the strain data from the MTS Alliance RT-30 test machine as a displacement load into the computation software, thus fully simulating the tensile test experiment. Please note that the model does not provide failure of the structure (Fig. 4). This is a fully acknowledged fact, as the model will need to incorporate additional algorithms to provide an accurate solution in the area of failure. This approach is the subject of our further efforts and the presented model is in the middle stage of its development.

5. Conclusions

The macromechanical tests have been conducted as a pilot experiment and cannot be therefore compared with other authors. The compression tests have proven to be more diverse due to the yet unclear nature of the deformation of the trabecular structure. The mean Young's modulus E of the trabecular specimens calculated from the linear part of the loading curves of the stress-strain diagrams is E_{ten} = 974.26 MPa for the tensile test and E_{comp} = 960.68 MPa for the compression test.

As predicted, the analysis showed that incorporating the trabecular structure has great effect on lowering the Young's modulus E of the whole structure. As opposed to regularly produced Ti-6Al-4V implants, where values of E are approximately 110 GPa, the values of E of the trabecular implant are below 1 GPa. This is a very significant reduction and the results are still to be compared with other experiments.

Further effort has been made to develop a material model which describes the trabecular structure. This model has been tuned to accurately represent the stress-strain diagram of the tensile test specimens. The geometry of the numerical model corresponds with dimensions of the real specimens. With this model developed, the next goal will be to incorporate failure of the structure and introduce a FEM model of a whole implant, which contains both trabecular and homogeneous cross-sections (Fig. 5) and will ultimately describe the nature of the mechanical behavior of the whole implant.

Fig. 5: Specimens (left) and structure composition (right) of the final implant for future analyses.

Acknowledgment

The financial support provided by SGS project application registered as OHK1-031/17 is gratefully acknowledged.

References

Aouni, E. et al. (2014) Physical and mechanical characterisation of 3D-printed porous titanium for biomedical applications, J Mater Sci., 25, pp. 2471-2480.

Dabrowski, B. et al. (2010) Highly porous titanium scaffolds for orthopaedic applications, J Biomed Mater Res, 95B, pp. 53-61.

Hartmann-H'Lawatscheck, T. (2015) Metal Laser Melting, Laser Technik Journal, 12, pp. 41-43.

Jíra, A. and Denk, F. (2016) Micromechanical analysis of dental implants and their surface modification, App. mech and mat., 827, pp. 367-370.

Niinomi, M. (1998) Design and mechanical properties of new b type titanium alloys for implant materials, Materials Science and Engineering, A243, pp. 244-249.

Niinomi, M. (1998) Mechanical properties of biomedical titanium alloys, Materials and Science Engineering, A243, pp. 231-236.

Řehounek, L., Denk, F. and Jíra, A. (2016) Trabecular structures of dental implants formed by 3D printing and their mechanical properties, 54th International Conference on Experimental Stress Analysis, EAN 2016; Hotel Srni, Srni; Czech Republic; 30 May 2016 through 2 June 2016; Code 123122.

Wiria, F.E. et al. (2010) Printing of Titanium implant prototype, Materials & Design, 31, pp. 101-105.